

Impurity-satellite ^{27}Al nuclear magnetic resonance in the f -site diluted non-Fermi-liquid alloys $\text{U}_{1-x}\text{La}_x\text{Pd}_2\text{Al}_3$

M. S. Rose, D. E. MacLaughlin, and B. -L. Young*

Department of Physics, University of California, Riverside, California 92521, USA

O. O. Bernal

Department of Physics and Astronomy, California State University, Los Angeles, California 90032, USA

V. Zapf,* E. Freeman, and M. B. Maple

Department of Physics, University of California, San Diego, La Jolla, California 92093, USA

(Received 23 January 2005; revised manuscript received 10 May 2005; published 11 July 2005)

Magnetic susceptibility and ^{27}Al nuclear magnetic resonance data are reported for the non-Fermi-liquid (NFL) alloys $\text{U}_{1-x}\text{La}_x\text{Pd}_2\text{Al}_3$, $x=0.8, 0.9$, and 1.0 . Ten percent doping of the lanthanum sites with uranium impurities shifts the resonance frequency of ^{27}Al nuclei near the U ions sufficiently such that satellite lines are resolved from the bulk line. The extra broadening of these satellite lines in $\text{U}_{0.1}\text{La}_{0.9}\text{Pd}_2\text{Al}_3$ is evidence for inhomogeneity in the magnetic susceptibility, and agrees with the NFL Kondo disorder model (KDM) and the Griffiths-McCoy phase model (GMPM) theories. However, the resulting distributions of characteristic energies do not extend down to zero, where uncompensated spins at finite temperatures would give rise to NFL behavior. This is evidence that the distribution of energies is not broad enough to be the cause of NFL behavior as described by the KDM and GMPM.

DOI: [10.1103/PhysRevB.72.014423](https://doi.org/10.1103/PhysRevB.72.014423)

PACS number(s): 75.40.Cx, 71.10.Hf, 76.60.Cq, 75.30.Mb

I. INTRODUCTION

A number of metals have been discovered in which the physical properties do not follow traditional Fermi liquid (FL) theory¹ (for a review see Ref. 2). Non-Fermi-liquid (NFL) behavior is seen in the transport [$\rho = \rho_0 + a(T/T_0)^n$, $n \lesssim 1.5$], thermodynamic, and magnetic [$C/T \propto \chi \propto -\ln(T/T_0)$ or $C/T \propto \chi \propto T^{-1+\lambda}$, $0 < \lambda < 1$] properties of these materials.² No theory has been found to date that can adequately describe the properties of all NFL alloys. Theories that have had success in describing the physical properties of a few systems are based on (a) proximity in the phase diagram to a quantum critical point (QCP),³⁻⁵ (b) magnetic disorder,⁵⁻⁷ and (c) multiple channels through which conduction electrons can screen magnetic impurities.^{8,9}

We have carried out magnetic susceptibility measurements and ^{27}Al nuclear magnetic resonance experiments in $\text{U}_{1-x}\text{La}_x\text{Pd}_2\text{Al}_3$. The electrical resistivity and specific heat of $\text{U}_{1-x}\text{La}_x\text{Pd}_2\text{Al}_3$ ($x=0.8$ and 0.9) have previously been determined¹⁰ to exhibit NFL behavior. The magnetic susceptibility has a Curie-Weiss-type temperature dependence, but its field dependence at low temperatures does not follow the expected Brillouin function for parameters obtained from the Curie-Weiss fits. The agreement is improved if a disordered energy scale (Curie-Weiss temperature) is assumed, as suggested by disorder-driven NFL models such as the Kondo disorder model (KDM) (Refs. 6 and 7) and the Griffiths-McCoy phase model (GMPM).^{5,11} However, the resulting energy distributions found from fits of the respective models to the magnetic susceptibility do not extend down to zero Kelvin, which is necessary in the KDM or GMPM models so that uncompensated spins or clusters at finite temperatures give rise to NFL behavior.

Nuclear magnetic resonance (NMR) has the ability to test disorder-driven models, as nuclear spins sample the local magnetic environment and are sensitive to inhomogeneity. A change in the NMR resonance frequency can originate from nearby magnetic ion(s) that contribute to the magnetic field felt by the NMR nuclei. If this effect is significant, *impurity satellite* lines¹² will develop in a dilute magnetic alloy, with the weight of each impurity satellite line determined by the number of nearby magnetic ions. These impurity satellite lines and the bulk line are both broadened by a magnetically disordered environment; a distribution of magnetic environments felt by the NMR nuclei is revealed by a distribution of resonances or an increase in the width of the NMR resonance line.

Liu *et al.*¹³ reported impurity satellite NMR measurements on the related NFL alloy $\text{U}_{1-x}\text{Th}_x\text{Pd}_2\text{Al}_3$. They concluded that the narrow lines observed at low temperature were indicative of a system in which disorder was not the driving mechanism for NFL behavior. Unlike the tetravalent thorium-doped system, however, trivalent elements such as yttrium or lanthanum may introduce significant electrical disorder upon substitution with tetravalent uranium. *A priori*, it is unclear whether the disorder introduced by the difference in dopant valency will have large enough effects to produce or strongly influence disorder-driven NFL behavior. This paper presents evidence that, although the KDM and the GMPM provide consistent descriptions of the inhomogeneous susceptibility in $\text{U}_{1-x}\text{La}_x\text{Pd}_2\text{Al}_3$, there is not enough inhomogeneity to explain the NFL behavior. Thus, it appears that the difference in dopant valency does not create enough disorder to be the dominating mechanism for NFL behavior in $\text{U}_{1-x}\text{La}_x\text{Pd}_2\text{Al}_3$. We also conclude that neither the presence nor the absence of a nearby QCP (as in $\text{U}_{1-x}\text{La}_x\text{Pd}_2\text{Al}_3$ and

$U_{1-x}Th_xPd_2Al_3$, respectively) produces agreement between disorder-driven NFL models and experimental data in the doped UPd_2Al_3 alloy.

Details of the preparation of aligned-powder $U_{1-x}La_xPd_2Al_3$ samples and techniques involved in obtaining data are discussed in Sec. II. In Sec. III A anisotropic magnetic susceptibility data are fit to various models assuming both spatially uniform and disordered energy scales. Section III B reviews energy and magnetic susceptibility probability distributions from disorder-driven NFL models, and Sec. III C addresses the relationship between NMR Knight shifts and widths to single-ion susceptibility. In Sec. IV predictions of the corresponding NMR line shapes are compared to ^{27}Al NMR spectra, and a temperature-dependent study of the NMR linewidth with respect to the average frequency of resonance is presented. Conclusions are given in Sec. V.

II. EXPERIMENT

The $U_{1-x}M_xPd_2Al_3$ systems, $M=Y, La,$ and Th , crystallize in the hexagonal $PrNi_2Al_3$ structure (space group $P6/mmm$) with all of the aluminum ions in crystallographically equivalent sites. $U_{0.1}La_{0.9}Pd_2Al_3$ and $U_{0.15}Y_{0.85}Pd_2Al_3$ samples were prepared by arc melting the constituent elements on a copper hearth in a high purity argon atmosphere.¹⁰ Each of the samples was then annealed at 900 °C for 7 days. The samples were then crushed to a size of 90 microns. The samples were mixed with Stycast 1266 epoxy and the powder particles were field aligned using the method for aligning magnetic “easy-plane” crystallites.¹⁴ A Quantum Design MPMS was used to make dc magnetization measurements for temperatures ranging between 5 and 300 K at 22.5 kG, and fields between 0 and 55 kG at 2 K. ^{27}Al pulsed NMR spectra were taken on a homemade pulsed homodyne spectrometer for temperatures between 5 and 270 K and frequencies between 15 and 80 MHz, using the field-swept frequency-shifted and summed technique.¹⁵

NMR spectra were obtained from samples of $U_{0.15}Y_{0.85}Pd_2Al_3$ and $U_{1-x}La_xPd_2Al_3, x=0.8, 0.9,$ and 1.0 for applied field H both parallel and perpendicular to the hexagonal c axis. Most data were taken for $x=0.9$, and a complete analysis was carried out only for this La concentration. However, the similarity of the spectra for $x=0.9$ and 0.8 , in particular the clear separation of the impurity satellite lines from the central transition (inset of Fig. 1), is good evidence that our conclusions apply for both concentrations. An example is shown in Fig. 1. The quadrupolar satellites of $U_{0.1}La_{0.9}Pd_2Al_3$ in Fig. 1 were identified¹⁶ and employed to determine the quadrupolar frequency ν_Q and asymmetry parameter η . Comparing first-order quadrupole transitions at 22.5 kG and 70.78 K for $H \parallel c$ of the crystallites gives $\nu_Q = 0.981 \pm 0.006$ MHz. Having determined ν_Q, η was determined by comparing the difference in resonance positions of the powder pattern extrema for $H \perp c$ at a number of fields. This was done at 44.7 K for $U_{0.1}La_{0.9}Pd_2Al_3$, and yields $\eta = 0.274 \pm 0.002$. These values of η and ν_Q are slightly higher than those found using NQR (nuclear quadrupole resonance)¹⁷ ($\eta=0.2$ and $\nu_Q=0.885$ MHz) and NMR (Ref. 18) ($\eta=0.22$ and $\nu_Q=0.949$ MHz) in the parent compound

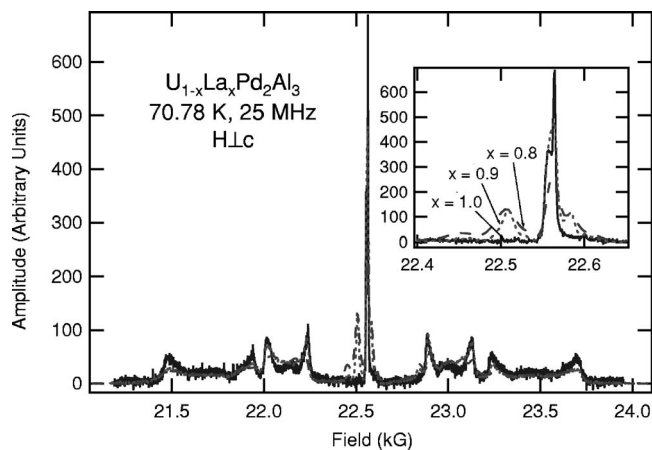


FIG. 1. NMR spectra of $U_{1-x}La_xPd_2Al_3, x=0.8, 0.9,$ and 1.0 . The quadrupolar satellites show a two-dimensional powder pattern due to random orientations of the crystallites in the basal plane along with the development of impurity satellite lines with increasing U concentration. Inset: Central transitions showing the development of impurity satellite lines with increasing U concentration.

UPd_2Al_3 . Because the quadrupolar splitting is large, the impurity satellite lines of the central transition do not overlap the quadrupole satellites over a broad field range.

For a statistical distribution of impurities, the impurity satellite intensities for different near-neighbor impurity configurations are given by a binomial distribution.¹² While the impurity satellite intensities of the lanthanum-doped alloys could be modeled by this binomial distribution, the spectra from the yttrium-doped alloy could not. This indicates a non-statistical impurity distribution (clustering, second-phase formation, etc.). We therefore cannot reliably know the origin of the observed Knight shift and NMR cannot show the cause of the NFL behavior in the $U_{1-x}Y_xPd_2Al_3$ system.

III. RESULTS AND DISCUSSION

A. Magnetic susceptibility: Fits assuming a homogeneous system

The temperature dependence of the magnetic susceptibility (M/H , where M is the magnetization) of $U_{0.1}La_{0.9}Pd_2Al_3$ was measured with $H \perp c$. The data were fit to a Curie-Weiss form $\chi = N\mu_B^2 p^2 / [3k_B(T+T_0)]$. This fit, shown in Fig. 2, results in an effective moment $p = 2.590 \pm 0.005 \mu_B$ and characteristic temperature $T_0 = 30.1 \pm 0.2$ K. A Curie-Weiss form for the low-temperature susceptibility does not agree with FL theory, which predicts $\chi(T) = \chi(0) - AT^2$, so that the good fit to the Curie-Weiss form is evidence for NFL behavior.

For further comparison with these data, temperature dependencies of the low- and high-temperature regimes for the single-ion susceptibility have been calculated using a Bethe ansatz solution to the $s-d$ model for $S=1/2$.¹⁹⁻²¹ The intermediate-temperature regime is well approximated by interpolating between the low- and high-temperature regimes of Wilson’s numerical renormalization group model using a Curie-Weiss form.^{21,22} Heavy-fermion or concentrated Kondo systems are at best only qualitatively described by the

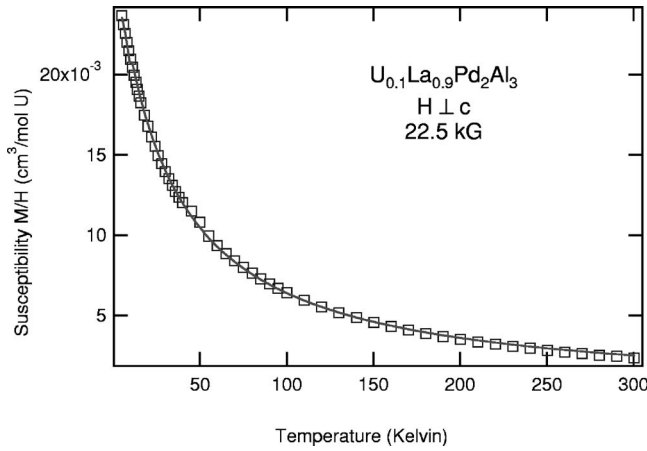


FIG. 2. Temperature dependence of the magnetic susceptibility in a field-aligned powder of $\text{U}_{0.1}\text{La}_{0.9}\text{Pd}_2\text{Al}_3$ with a field of 22.5 kG applied perpendicular to the c axis. Curve: Curie-Weiss fit with effective moment of $p=2.590\pm 0.005 \mu_B$ and characteristic $T_0=30\pm 0.2$ K.

s - d model, so an analysis based on these formulas must be thought of as phenomenological.

The dependence of the single-ion Kondo susceptibility $\chi_{\text{imp}}(T)$ on the ratio of the temperature to the Kondo temperature $x=T/T_K$ may be written as

$x=0$:

$$\chi_{\text{imp}}(0) = \frac{w(g\mu_B)^2}{4k_B T_K}, \quad (1)$$

$x < 0.5$:

$$\chi_{\text{imp}}(x) = \chi_{\text{imp}}(0) \left[1 - \frac{\sqrt{3}\pi^3 w^2 x^2}{4} \right], \quad (2)$$

$0.5 < x < 16$:

$$\chi_{\text{imp}}(x) = \frac{0.68\chi_{\text{imp}}(0)}{w(x + \sqrt{2})}, \quad (3)$$

$x > 16$:

$$\chi_{\text{imp}}(x) = \frac{\chi_{\text{imp}}(0)}{wx} \left[1 - \frac{1}{\ln(x)} \right], \quad (4)$$

where $w=0.41072$ is the Wilson number²³ and g is the Landé factor of the f ion.

Fits of these single-ion Kondo susceptibility expressions (each in the appropriate previously stated temperature regimes) to the data, shown in Fig. 3, give characteristic temperatures of 20.3 and 47 K for a magnetic field of 22.5 kG applied perpendicular and parallel to the c axis, respectively (The small anomaly at roughly 45 K for H - c is not thought to be intrinsic, and probably arises from the antiferromagnetic transition of a small amount of frozen molecular oxygen in the magnetometer.). These values are slightly higher than those found via resistivity measurements ($T_0 \approx 17$ K),¹⁰ but consistent with the values determined from the orientationally-averaged susceptibility and the heat capacity ($T_0 \approx 30$ K).¹⁰ Thus, $\chi(T)$ can be fit to both Fermi-liquid and

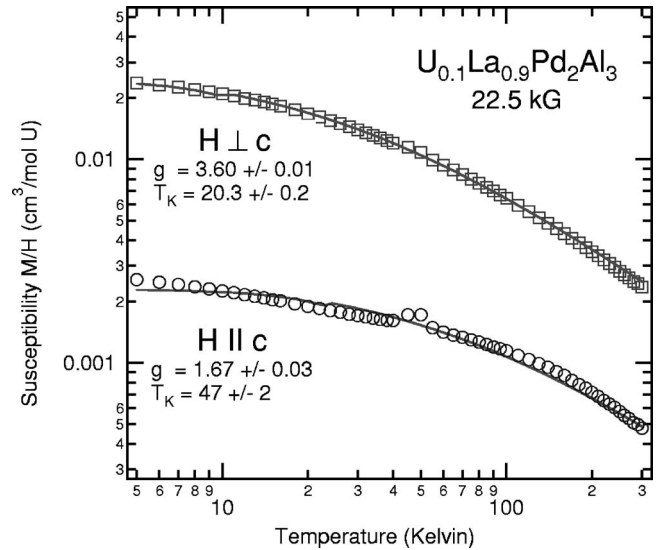


FIG. 3. Magnetic susceptibility measurements taken along and perpendicular to the c axis of the crystal. Solid curves: Fits to the single-ion Kondo susceptibility.

NFL (Curie-Weiss) functional forms, and by itself does not indicate the appropriate picture.

Figure 4 shows the field dependence of the susceptibility M/H for $H \perp c$, together with the Brillouin function susceptibility

$$\chi = M/H = NgJ\mu_B B_J(x)/H,$$

where

$$B_J(x) = \frac{2J+1}{2J} \coth \frac{2J+1}{2J} x - \frac{1}{2J} \coth \frac{1}{2J} x,$$

and

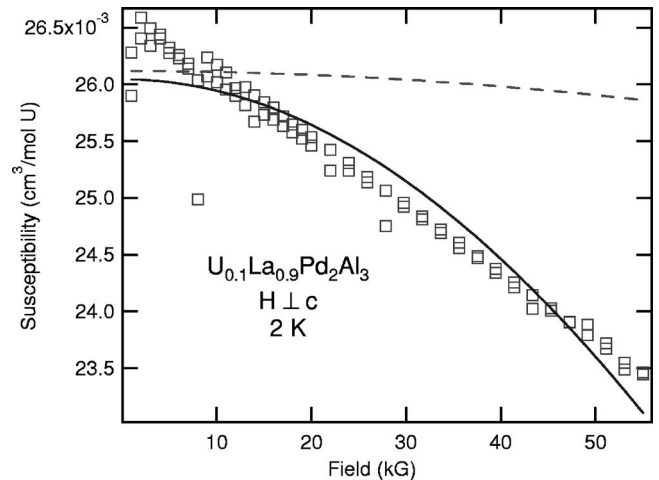


FIG. 4. Susceptibility measurements (open squares) taken at $T=2$ K with the applied magnetic field perpendicular to the c axis of the crystal. Dashed curve: Brillouin function susceptibility for $p=2.590\pm 0.005 \mu_B$, $T_K=30$ K (parameters from Curie-Weiss fit) and $J=0.5$. Solid curve: Brillouin function susceptibility for $p=4.72 \mu_B$, $T_K=26.8$ K with best fit for an angular momentum $J=0.90$ (parameters from disorder-driven model fit).

$$x = \frac{gJ\mu_B H}{k_B(T + T_0)}. \quad (5)$$

The parameters used to plot the dashed curve in Fig. 4 were determined from the Curie-Weiss temperature dependence and J was taken to be $1/2$, which is the smallest physical value (an unphysically small value of J produces better agreement with the data). As described below in Sec. III B, the inhomogeneous susceptibility predicted by both disorder-driven models studied in this paper produces the field-dependent susceptibility shown by the solid curve in Fig. 4. This gives a more physical result for the angular momentum ($J=0.90\pm 0.01$ when allowed to vary for best fit).

Thus, the field dependence of the low-temperature susceptibility disagrees with a single- T_0 picture, and is in better agreement with the disorder-driven scenarios.

B. Probability distributions for disorder-driven NFL models

The disorder-driven models assume that the energy scale for the alloy (Kondo temperature in the Kondo disorder model, KDM,^{6,7} cluster energy in the Griffiths-McCoy phase model, GMPM,^{5,11}) is not spatially uniform, but is distributed. In order to find the spatial average susceptibility $\bar{\chi}(T)$, one must integrate over the distribution function $P(\mathcal{E})$ for the disordered energy parameter \mathcal{E}

$$\bar{\chi}(T) = \int_0^\infty \chi(T, \mathcal{E}) P(\mathcal{E}) d\mathcal{E}, \quad (6)$$

where $\chi(T, \mathcal{E}=T_K)$ is the susceptibility for fixed \mathcal{E} . In the KDM $\chi(T, \mathcal{E})$ is the single- T_K Kondo susceptibility, which we take to be given by Eqs. (1)–(4). The distributed parameter is the Kondo temperature $T_K = T_F \exp(-1/|\mathcal{J}\rho_0|)$, where \mathcal{J} is the exchange coupling constant, ρ_0 is the density of states of the Fermi surface, and T_F is the Fermi temperature. An assumed Gaussian distribution of $\mathcal{J}\rho_0$ gives⁶

$$\begin{aligned} P(\mathcal{E}) &= P(T_K) \\ &= \frac{1}{\sqrt{2\pi w T_K}} \frac{1}{\ln(T_K/T_F)^2} \\ &\times \exp\left[\frac{-1}{2w^2} \left(\frac{-1}{\ln(T_K/T_F)} - \overline{\mathcal{J}\rho_0}\right)^2\right], \end{aligned} \quad (7)$$

where $\overline{\mathcal{J}\rho_0}$ is the average coupling strength and w is the width of the coupling strength distribution.

For the GMPM the distributed parameter is the cluster energy E , which is inversely correlated with the size of the cluster. The probability distribution $P(E)$ for the cluster energies is²⁴

$$P(\mathcal{E}) = P(E) = \begin{cases} (\lambda/\epsilon_0)(E/\epsilon_0)^{(\lambda-1)}, & 0 < E < \epsilon_0, \\ 0, & E > \epsilon_0, \end{cases} \quad (8)$$

where ϵ_0 is a cutoff energy and λ is a nonuniversal exponent; $\lambda < 1$ describes singular (NFL) behavior.

Fits of the average susceptibility [Eq. (6)] for the KDM and GMPM to the data for $\mathbf{H} \perp \mathbf{c}$ are shown in Fig. 5. The value of the reduced statistical χ^2 for the disorder-model fits

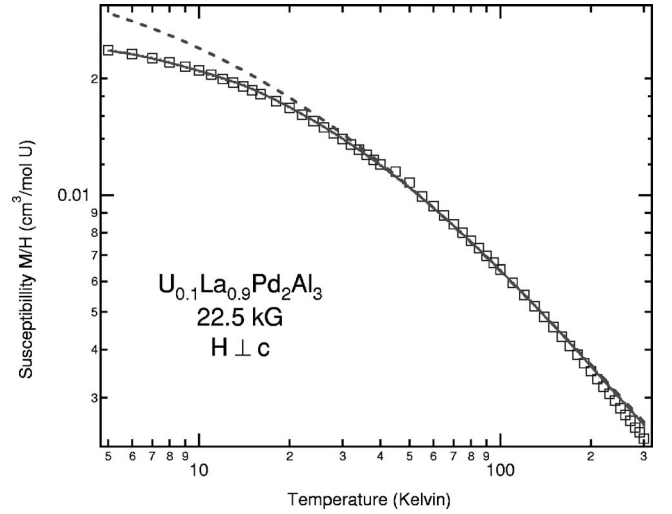


FIG. 5. Temperature dependence of the magnetic susceptibility at 22.5 kG. Fits of the KDM and GMPM are plotted over the susceptibility data. At these temperatures and this field it is impossible to distinguish between the two models. Dashed curve: example of NFL behavior observed when distribution of the Kondo temperature is forced to be large ($w=0.02$).

is a factor of 2 better than for fits to the single-ion Kondo susceptibility of Eqs. (1)–(4). A summary of the fit parameters is given in Table I.

The GMPM fit value of $\lambda=4.0$ establishes that this model does not account for the NFL behavior observed in $U_{0.1}La_{0.9}Pd_2Al_3$. NFL behavior only occurs for $\lambda < 1$, for which a divergence is obtained at $T=0$. This leads to corresponding divergences in the magnetic susceptibility and heat capacity. Using the fit parameters from Table I, $P(\mathcal{E})$ has been calculated directly using Eqs. (7) and (8) for the KDM and the GMPM, respectively, and is given in Figs. 6 (KDM) and 7 (GMPM). These figures show that $P(\mathcal{E})$ does not have any appreciable weight near $\mathcal{E}=0$ for either model. Little or no weight at low energies means that, even though the disorder is quite observable, it is not strong enough to cause NFL behavior.^{5,7,25} As an example, the dashed curve in Fig. 6 gives the Kondo-disorder $P(T_K)$ for a larger value of $w=0.02$, so that weight is transferred to lower values of T_K . It can be seen in Fig. 5 that the corresponding susceptibility disagrees strongly with the experimental data. The fit shows, therefore, that there is little weight of $P(E)$ for small values of E .

C. ²⁷Al impurity satellite knight shifts and linewidths

While the disorder-driven models are not able to explain NFL behavior based on fits to the magnetic susceptibility, we

TABLE I. Parameters of disorder-driven model fits to magnetic susceptibility at 22.5 kG with the NMR field applied perpendicular to the \mathbf{c} axis of the crystal.

KDM	GMPM
$g=3.62\pm 0.01$	$g=3.62\pm 0.01$
$\overline{\mathcal{J}\rho_0}=0.162\pm 0.001$	$\lambda=4.00\pm 0.45$
$w=0.0065\pm 0.0013$	$\epsilon_0=26.8\pm 1.0$

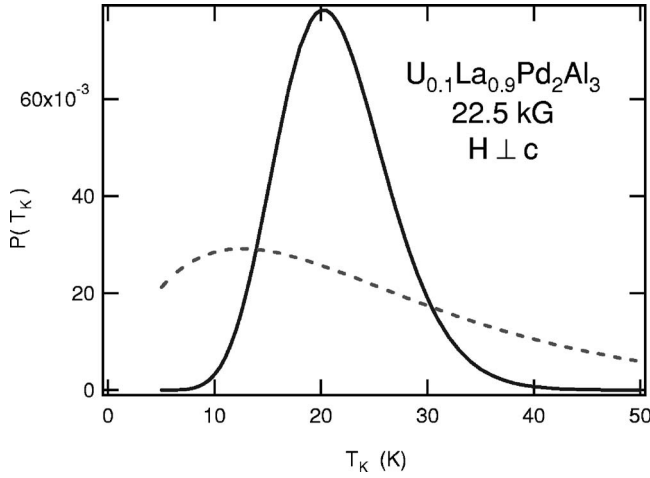


FIG. 6. Solid curve: Distribution function $P(T_K)$ based on the fit of Fig. 5 and the assumption of a Gaussian distribution of coupling constants as described by the KDM [Eq. (7)]. Dashed curve: example of distribution of Kondo temperatures ($w=0.02$) which result in NFL behavior.

argue in this section that they do roughly predict the Knight shifts and spread in Knight shifts observed using NMR. The sample-average Knight shift is related to the sample-average single ion susceptibility $\bar{\chi}$ by $\bar{K} = a\bar{\chi}$ (Ref. 16) if we assume that (a) all nuclei in crystallographically equivalent sites have the same value of $a \equiv \sum_j a_{ij}$, where a_{ij} is the hyperfine coupling constant between the i th NMR nucleus and the j th impurity moment, and (b) any disorder in a_{ij} and the susceptibility are independent of each other. Similarly, the mean square width of the Knight shift distribution may be written²⁶

$$\overline{\delta K_i^2} = \sum_{j,k} a_{ij} a_{ik} \overline{\delta \chi_j \delta \chi_k}, \quad (9)$$

where the sum is over all U ions that are coupled to the nucleus.

Upon doping with the magnetic uranium ion [$\text{U}_{1-x}\text{La}_x\text{Pd}_2\text{Al}_3$, $x=0.8$ and 0.9], the NMR bulk line and impurity satellite¹² weights are determined by the binomial distribution

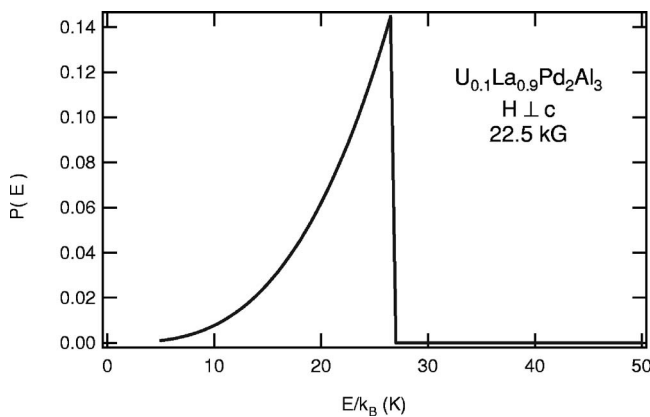


FIG. 7. Distribution function $P(E)$ based on the fit of Fig. 5 and the GMPM probability distribution [Eq. (8)].

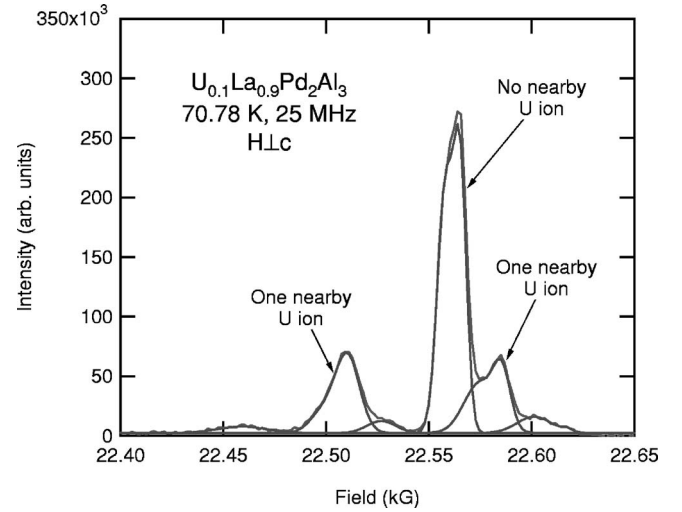


FIG. 8. NMR spectra of $\text{U}_{0.1}\text{La}_{0.9}\text{Pd}_2\text{Al}_3$ central transitions. Asymmetric line shapes used to model varying number of nearby U ions in the two closest shells to the NMR nuclei. The weights of the bulk and satellite lines are determined by the concentration of uranium via the binomial distribution. Unlabeled peaks origins are low probability concentrations of uranium near NMR nuclei.

$$W(N_1) = \frac{N!}{N_1! (N - N_1)!} p^{N_1} (1 - p)^{N - N_1}, \quad (10)$$

where, for a concentration p of magnetic ions, $W(N_1)$ is the probability of finding a given number N_1 of magnetic ions in a shell surrounding the NMR nuclei capable of holding N ions. Because of the long-range nature of the Ruderman-Kittel-Kasuya-Yosida (RKKY) interaction between the doped magnetic ions and the NMR nuclei, magnetic ions in sites beyond the nearest-neighbor sites may contribute to the probability distribution.

In $\text{U}_{1-x}\text{La}_x\text{Pd}_2\text{Al}_3$ the nearest-neighbor and next-nearest-neighbor site distances are about 1 \AA apart and both produce resolved impurity satellites. Each shell contains four sites. Ten percent doping of U would require 19% of the total weight of the NMR spectra to make up each peak originating from only one U ion in that particular shell. These lines are the lines at 22.51 and 22.58 kG in the insets to Fig. 1 and Fig. 8, respectively. Over all temperatures and fields investigated in this study, the peaks labeled “one nearby U ion” in Fig. 8 were successfully modeled with 18% of the total weight of the NMR spectra. The data do not determine which satellite is due to which shell; however, this is not crucial to our analysis.

In the case of only one uranium ion coupled to the NMR nucleus only one term in Eq. (9) is needed, i.e.,

$$\delta K^2 = a^2 \delta \chi^2. \quad (11)$$

The value of a can be determined from the slope of a Clogston-Jaccarino plot (Knight shift vs susceptibility), which should be linear. For the low-field impurity satellite in Fig. 8, this is indeed the case, as shown in Fig. 9, and gives $a = (28.14 \pm 0.15) \% / (\text{cm}^3 / \text{mol U})$. The fact that the Clogston-Jaccarino plot is linear over the entire temperature

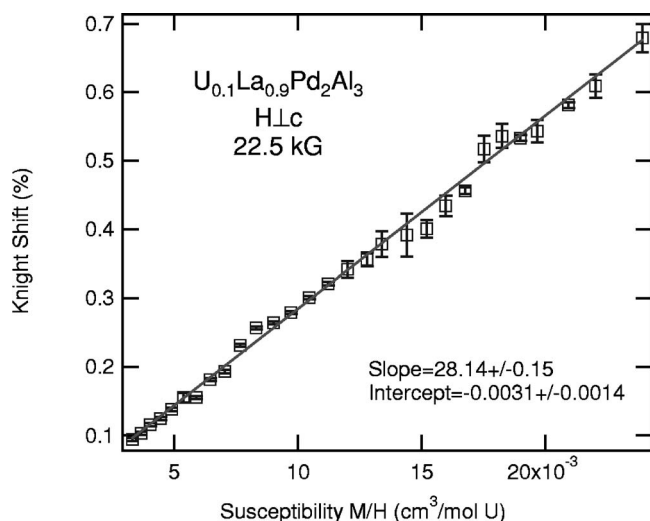


FIG. 9. Clogston-Jaccarino plot of ^{27}Al Knight shift from NMR nuclei with one nearby magnetic ion (the low-field impurity satellite in Fig. 8) in $\text{U}_{0.1}\text{La}_{0.9}\text{Pd}_2\text{Al}_3$. Data taken at 22.5 kG with the magnetic field applied perpendicular to the c axis.

range (5–220 K) supports the assumption that disorder in the hyperfine coupling is independent of disorder in the average magnetic susceptibility. It also implies the temperature independence of the coupling constant a .

IV. DISORDER-DRIVEN NFL MODELS: PREDICTIONS OF NMR LINE SHAPES

Having determined the coupling constant a , the probability distributions $P(\mathcal{E})$, and the fit parameters given in Table I, comparison of NMR line shapes can be made with theoretical predictions of $P(\chi)$ from the disorder models. The probability distribution for the susceptibility $P(\chi) = |d\mathcal{E}/d\chi|P(\mathcal{E})$ is given for the KDM and the GMPM for a selection of temperatures in Figs. 10 and 11, respectively. NMR line shapes may be compared with these predicted distribution functions after normalizing the NMR spectra frequency shift scale by the coupling constant a [cf. Eq. (11)]. The main difference between the calculated probability distribution and the observed NMR spectra is broadening of the spectra by site-independent broadening mechanisms. The existence of this broadening is seen from the fact that aluminum ions with no nearby uranium ions experience a distribution of fields on the order of 10 Q at 22.5 kG and 70.78 K (Fig. 8). Broadening of the zero nearest-neighbor (Znn) line by distant magnetic impurities also broadens the impurity satellite lines in similar fashion.²⁷ Such broadening effects were removed by a deconvolution of the Znn “bulk” line from the impurity satellite lines. The shapes of the deconvoluted impurity satellite lines give the distribution function for the Knight shift (Fig. 13).

At low temperatures it was found that the deconvolution process did not produce significant spectral changes, due to the large difference in linewidth between the bulk line and the impurity satellite lines (cf. Fig. 12). Figures 14 and 15 show the KDM and GMPM calculations, respectively, com-

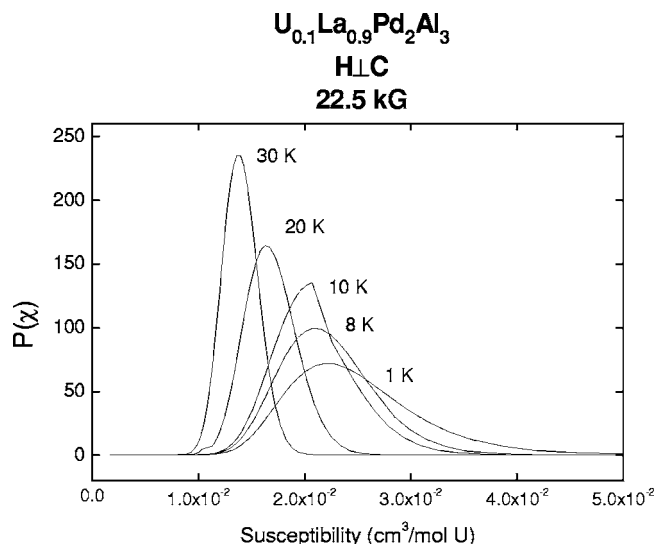


FIG. 10. Probability distribution for the magnetic susceptibility at 22.5 kG for select temperatures as predicted by the KDM. The discontinuous slope observed at 10 K is an artifact originating from the discontinuity in the single-ion Kondo susceptibility at the low-temperature crossover [Eqs. (2) and (3)].

pared to the deconvoluted NMR spectrum at 28 K and 22.5 kG. Neither model is able to reproduce the details of the NMR spectrum, but the rms widths of the susceptibility distributions for both models are observed to be in good agreement with the NMR spectrum with no further adjustable parameters.

This agreement suggests that the susceptibility distribution is due to a distribution of Kondo temperatures (cluster energies) as given by the KDM (GMPM). The value of the fractional spread in susceptibility $\delta\chi/\chi(T \rightarrow 0 \text{ K}) \approx 0.2\text{--}0.3$ (Fig. 16) is significantly less than 1, however, indicating that there is little weight at low characteristic energies.²⁵ Thus, the NMR measurements confirm our conclusions from analysis of the susceptibility data, namely, that disorder is not the

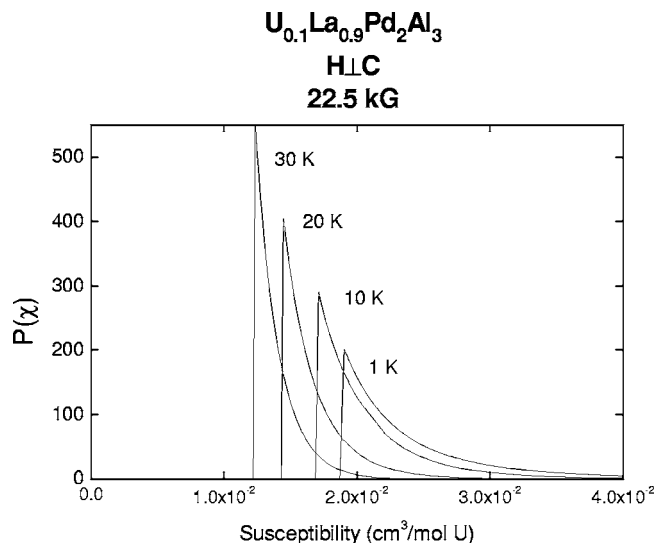


FIG. 11. Probability distribution for the magnetic susceptibility at 22.5 kG for select temperatures as predicted by the GMPM.

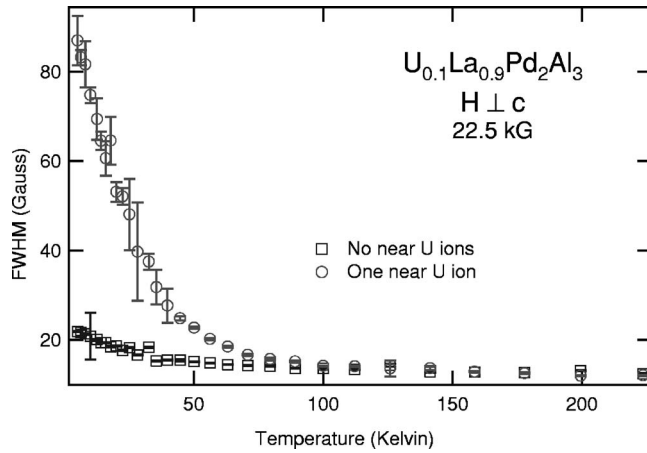


FIG. 12. FWHM of lines corresponding to NMR nuclei with zero and one near-neighbor uranium ion in $\text{U}_{0.1}\text{La}_{0.9}\text{Pd}_2\text{Al}_3$. Measurements taken at 22.5 kG and with the magnetic field applied perpendicular to the c axis.

driving mechanism for NFL behavior in $\text{U}_{1-x}\text{La}_x\text{Pd}_2\text{Al}_3$. In Fig. 16 there appears to be a slight change in slope in the plot of $\delta\chi/\chi$ vs χ below the mean Kondo temperature ($T_K = 20$ K, $\chi = 17$ $\text{cm}^3/\text{mol U}$); however, a fit of the entire data to a straight line, assuming the errors shown in Fig. 16, gives a χ^2 per degree of freedom of 0.206. Thus, the linear $\delta\chi/\chi$ vs χ behavior found in disorder-driven models for small $\delta\chi/\chi$ (Ref. 25) fits the data in $\text{U}_{0.1}\text{La}_{0.9}\text{Pd}_2\text{Al}_3$ to within experimental error.

V. CONCLUSIONS

Fits were made of the disorder-driven KDM and the GMPM to susceptibility data, incorporating the full single-ion Kondo susceptibility. A complete analysis was carried out only for $\text{U}_{0.1}\text{La}_{0.9}\text{Pd}_2\text{Al}_3$; however, the clear separation of the impurity satellite lines from the central transition (inset of Fig. 1) is good evidence that our conclusions apply for the

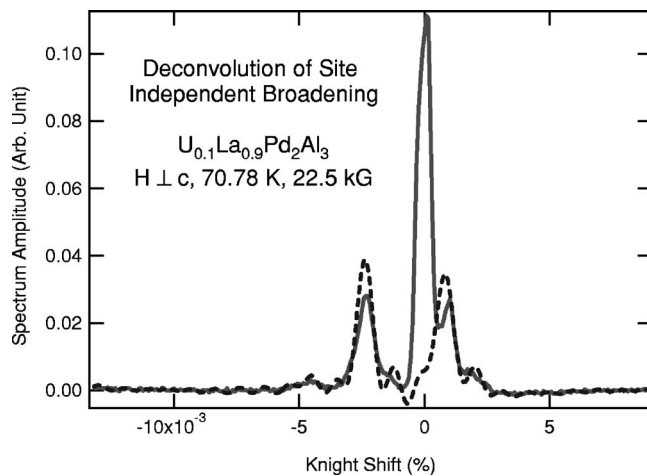


FIG. 13. Solid curve: As-measured NMR spectrum at 70.78 K and 22.5 kG. Dotted curve: Deconvolution of the Z_{nn} line from the solid line.

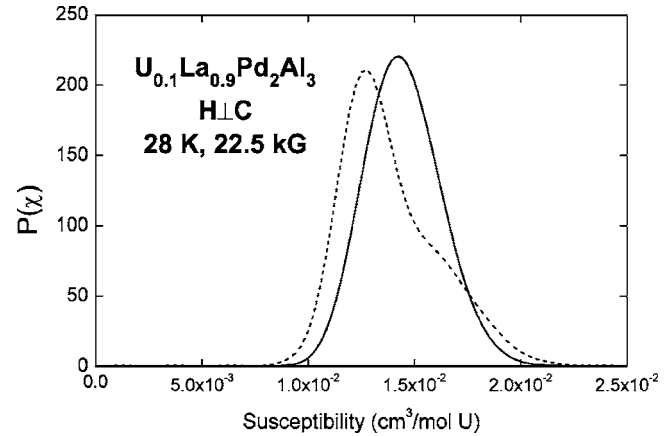


FIG. 14. The magnetic susceptibility probability distribution predicted by the KDM at 22.5 kG and 28 K for a single magnetic impurity (solid line) is compared with the corresponding NMR spectrum (dotted line) after removal of site independent broadening effects via deconvolution.

$x=0.8$ concentration as well. It was determined that, although both models fit the data, neither model can be considered the mechanism behind the NFL behavior in this alloy system. This is because the distributions of characteristic energies \mathcal{E} are found to be too narrow to provide appreciable weight at low \mathcal{E} , which is the criterion for having uncompensated spins at low temperatures and hence NFL behavior. Consistent with this general behavior, a fit of the GMPM to the susceptibility data found a value of exponent λ that is considerably greater than 1, i.e., out of the range of validity of the model ($\lambda \leq 1$).

A comparison of the low-field ^{27}Al impurity satellite Knight shift and the magnetic susceptibility yields a value of $a = 28.14 \pm 0.15\% / (\text{cm}^3/\text{mol U})$ for the hyperfine coupling constant. This determination allows direct comparison to be made between the distribution functions predicted by the disorder-driven models and deconvoluted NMR spectra. While the distribution functions do not exactly reproduce the

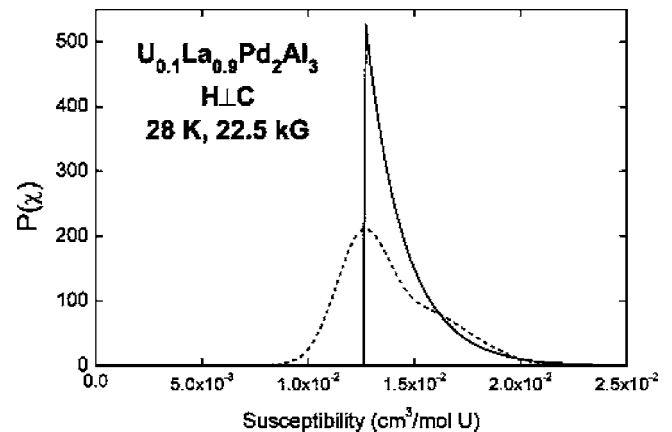


FIG. 15. The magnetic susceptibility probability distribution predicted by the GMPM at 22.5 kG and 28 K for a single magnetic impurity (solid line) is compared with the corresponding NMR spectrum (dotted line) after removal of site-independent broadening effects via deconvolution.

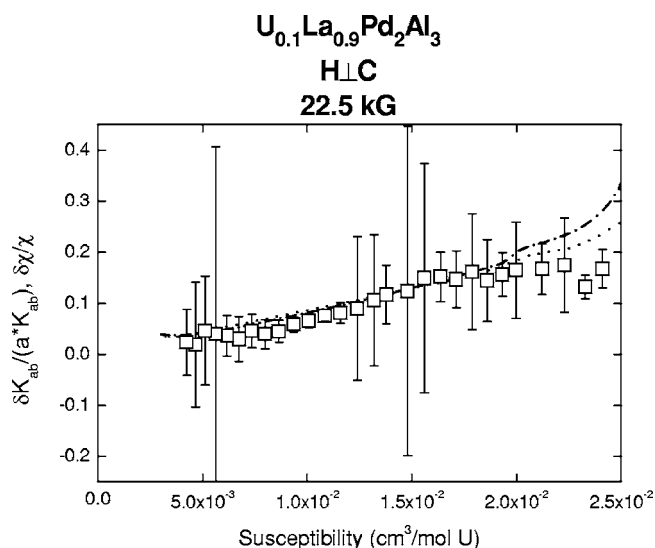


FIG. 16. Bernal plot showing the expected linear behavior of relative rms spread ($\delta\chi/\chi$) in inhomogeneous susceptibility increasing with increasing susceptibility χ . Dot-dash curve is the prediction of the GMPM, dotted curve is the prediction of the KDM, and the open squares are NMR measurements of disorder.

details of the NMR line shapes, it is found that the predictions of both disorder-driven NFL models of the average susceptibility and rms widths are in good agreement with the NMR data over the temperature range studied. The value of the fractional rms spread $\delta\chi/\chi$ approached at $T=0$ K (Fig. 16) is significantly less than 1, again indicating that the spread in the energy scale is insufficient to cause NFL behavior.²⁵ Thus, both susceptibility and NMR measure-

ments confirm that disorder is not the driving mechanism behind NFL behavior in this alloy.

NMR measurements have previously been carried out on $U_{0.1}Th_{0.9}Pd_2Al_3$,¹³ in which no QCP is observed in the phase diagram and the nonmagnetic dopant (Th) is tetravalent. Disorder-driven models are unable to describe the NFL behavior in this system, since here the NMR linewidths are significantly less than predicted by disorder-driven model fits to the susceptibility. This is in contrast to the present results in $U_{0.1}La_{0.9}Pd_2Al_3$, where the disorder-driven models are roughly able to describe both the susceptibility and the NMR spectra but give distribution widths that are too narrow to account for the NFL behavior. A comparison of these two systems suggests that disorder-driven models cannot describe the NFL behavior in doped UPd_2Al_3 regardless of the degree of proximity to a QCP (present in $U_{1-x}La_xPd_2Al_3$ but absent in $U_{1-x}Th_xPd_2Al_3$) or the valency of the nonmagnetic dopant. It is yet to be determined whether the trivalent nonmagnetic dopant or the proximity to a QCP in the lanthanum-doped system is responsible for the improved agreement between the disorder-driven models and NMR experiments as compared to the thorium-doped system.

ACKNOWLEDGMENTS

We are grateful to H. G. Lukefahr for help with sample preparation and for useful discussions. This research was supported by US NSF Grant Nos. DMR-9731361 and DMR-0102293 (UC Riverside), DMR00-72125 (UC San Diego), DMR0203524 (CSU Los Angeles), and US DOE Grant No. DE FG03-86ER-45230 (UC San Diego).

*Present address: Los Alamos, New Mexico 87545.

- ¹A. J. Leggett, *Rev. Mod. Phys.* **47**, 331 (1975).
- ²G. R. Stewart, *Rev. Mod. Phys.* **73**, 797 (2001).
- ³J. A. Hertz, *Phys. Rev. B* **14**, 1165 (1976).
- ⁴S. Sachdev, *Quantum Phase Transitions*, 1st ed. (Cambridge University Press, Cambridge, 1999).
- ⁵A. H. Castro Neto, G. Castilla, and B. A. Jones, *Phys. Rev. Lett.* **81**, 3531 (1998).
- ⁶O. O. Bernal, D. E. MacLaughlin, H. G. Lukefahr, and B. Andraka, *Phys. Rev. Lett.* **75**, 2023 (1995).
- ⁷E. Miranda, V. Dobrosavljević, and G. Kotliar, *J. Phys.: Condens. Matter* **48**, 9871 (1996).
- ⁸P. Nozières and A. Blandin, *J. Phys. (France)* **41**, 193 (1980).
- ⁹P. Schlottmann and P. D. Sacramento, *Adv. Phys.* **42**, 641 (1993).
- ¹⁰V. S. Zapf, R. P. Dickey, E. J. Freeman, C. Sirvent, and M. B. Maple, *Phys. Rev. B* **65**, 024437 (2002).
- ¹¹A. H. Castro Neto and B. A. Jones, *Phys. Rev. B* **62**, 14975 (2000).
- ¹²J. B. Boyce and C. P. Slichter, *Phys. Rev. B* **13**, 379 (1976).
- ¹³C. Y. Liu, D. E. MacLaughlin, H. G. Lukefahr, G. Miller, K. Hui, M. B. Maple, M. C. de Andrade, and E. J. Freeman, *Phys. Rev. B* **62**, 430 (2000).
- ¹⁴B. L. Young, M. S. Rose, D. E. MacLaughlin, K. Ishida, O. O. Bernal, H. G. Lukefahr, K. Heuser, E. J. Freeman, and M. B. Maple, *Rev. Sci. Instrum.* **73**, 3038 (2002).
- ¹⁵W. G. Clark, M. E. Hanson, F. Lefloch, and P. Segransan, *Rev. Sci. Instrum.* **66**, 2453 (1995).
- ¹⁶G. C. Carter, L. H. Bennett, and D. J. Kahan, *Prog. Mater. Sci.* **20** (1977).
- ¹⁷Y. Kohori and T. Kohara, *Physica B* **199–200**, 135 (1994).
- ¹⁸M. Kyogaku, Y. Kitaoka, K. Asayama, C. Geibel, C. Schank, and F. Steglich, *J. Phys. Soc. Jpn.* **62**, 4016 (1993).
- ¹⁹N. Andrei, *Phys. Rev. Lett.* **45**, 379 (1980).
- ²⁰P. B. Wiegmann, *Sov. Phys. JETP* **31**, 392 (1980).
- ²¹A. C. Hewson, *The Kondo Problem to Heavy Fermions* (Cambridge University Press, Cambridge, 1993).
- ²²P. B. Wiegmann and A. Tselik, *J. Phys. C* **12**, 2281 (1983).
- ²³N. Andrei and J. H. Lowenstein, *Phys. Rev. Lett.* **46**, 356 (1981).
- ²⁴C. Y. Liu, D. E. MacLaughlin, A. H. Castro Neto, H. G. Lukefahr, J. D. Thompson, J. L. Sarrao, and Z. Fisk, *Phys. Rev. B* **61**, 432 (2000).
- ²⁵O. Bernal, D. E. MacLaughlin, A. Amato, R. Feyerherm, F. N. Gyax, A. Schenck, R. H. Heffner, L. P. Le, G. J. Nieuwenhuys, B. Andraka, H. v. Löhneysen, O. Stockert, and H. R. Ott, *Phys. Rev. B* **54**, 13000 (1996).
- ²⁶D. E. MacLaughlin, O. O. Bernal, and H. G. Lukefahr, *J. Phys.: Condens. Matter* **8**, 48 (1996).
- ²⁷R. E. Walsted and L. R. Walker, *Phys. Rev. B* **9**, 4857 (1974).